

1 **Heterologous vaccination regimens with self-amplifying RNA and Adenoviral**  
2 **COVID vaccines induce superior immune responses than single dose vaccine**  
3 **regimens in mice**

4

5

6 Alexandra J Spencer<sup>1\*</sup>, Paul F McKay<sup>2</sup>, Sandra Belij-Rammerstorfer<sup>1</sup>, Marta Ulaszewska<sup>1</sup>,

7 Cameron D Bissett<sup>1</sup>, Kai Hu<sup>2</sup>, Karnyart Samnuan<sup>2</sup>, Daniel Wright<sup>1</sup>, Hannah R Sharpe<sup>1</sup>, Ciaran

8 Gilbride<sup>1</sup>, Adam Truby<sup>1</sup>, Elizabeth R Allen<sup>1</sup>, Sarah C Gilbert<sup>1</sup>, Robin J Shattock<sup>2</sup>, Teresa

9 Lambe<sup>1</sup>

10

11 ***Affiliations:***

12 <sup>1</sup>*The Jenner Institute, Nuffield Department of Medicine, University of Oxford,*

13 *United Kingdom*

14 <sup>2</sup>*Department of Infectious Disease, Imperial College London, United Kingdom*

15

16 *\*Correspondence to: Alexandra J Spencer, The Jenner Institute, ORCRB, Roosevelt Drive,*

17 *Oxford OX3 7DQ. Email: alex.spencer@ndm.ox.ac.uk.*

18

19

20 **Short title:** Superior immunity with heterologous vaccination regimens

21

22 **Abstract**

23 Several vaccines have demonstrated efficacy against SARS-CoV-2 mediated disease, yet  
24 there is limited data on the immune response induced by heterologous vaccination  
25 regimens using alternate vaccine modalities. Here, we present a detailed description of the  
26 immune response, in mice, following vaccination with a self-amplifying RNA (saRNA) vaccine  
27 and an adenoviral vectored vaccine (ChAdOx1 nCoV-19/AZD1222) against SARS-CoV-2. We  
28 demonstrate that antibody responses are higher in two dose heterologous vaccination  
29 regimens than single dose regimens, with high titre neutralising antibodies induced.  
30 Importantly, the cellular immune response after a heterologous regimen is dominated by  
31 cytotoxic T cells and Th1<sup>+</sup> CD4 T cells which is superior to the response induced in  
32 homologous vaccination regimens in mice.

33

## 34 **Introduction**

35 A number of vaccines against SARS-CoV-2 have reached late-stage clinical trials with  
36 encouraging efficacy readouts and mass vaccination schemes already initiated across  
37 several countries. Multiple vaccine technologies are being advanced <sup>1</sup>, but there is limited  
38 information on how these vaccine modalities may work in combination. With ongoing  
39 clinical trial assessment of numerous SARS-CoV-2 vaccines and new mass vaccination  
40 incentives, there is a recognised real-world scenario where individuals may be vaccinated  
41 with different vaccine modalities. However, the utility of vaccination regimens combining  
42 different types of vaccine approaches remains to be determined.

43

44 Self-amplifying RNA (saRNA) typically encodes the alphaviral replicase and a target antigen.  
45 Upon entry into the cytoplasm, the RNA is amplified with subsequent translation of the  
46 target antigen <sup>2</sup>. The SARS-CoV-2 saRNA vaccine has been demonstrated to be highly

47 immunogenic in preclinical animal models <sup>3</sup> and is progressing through clinical trial  
48 assessment with promising results. Adenoviruses are a frequently used viral vector vaccine  
49 technology, they can be rapidly made to GMP at large scale, and a single vaccination can be  
50 sufficient to provide rapid immunity in individuals <sup>4</sup>. In particular, chimpanzee derived  
51 adenoviruses (ChAd) have good safety profiles, whilst inducing strong cellular and humoral  
52 immune response against multiple target disease antigens <sup>5-7</sup>. Previous studies have  
53 demonstrated efficacy after vaccination with ChAdOx1 nCoV-19/AZD1222 against SARS-  
54 CoV-2 mediated disease <sup>8</sup>, with concomitant high titre humoral immune responses and a  
55 measurable Th1-dominated cellular immune response <sup>9,10</sup>. Importantly, an immune profile  
56 consistently observed across different animal species <sup>11,12</sup>.

57

58 In this study, the immunogenicity of saRNA and ChAdOx1 vaccines expressing full-length  
59 SARS-CoV-2 spike protein were assessed in mice following vaccination with different vaccine  
60 modalities combination. We demonstrate robust antibody responses following  
61 heterologous vaccination regimens, with high titre neutralising antibodies. The cellular  
62 immune response is dominated by cytotoxic T cells secreting IFN $\gamma$  and TNF $\alpha$  and antigen  
63 specific CD4<sup>+</sup> T cells of a Th1 phenotype, with significantly higher antigen specific responses  
64 observed following heterologous vaccination than those responses induced in single vaccine  
65 regimens.

66

67

68

69

70

71 **Results**

72 **Heterologous vaccination potentiates SARS-CoV-2 spike-specific antibody response**

73 It was previously shown that homologous prime-boost immunization with saRNA<sup>3</sup> or ChAd  
74 <sup>11</sup> induced a SARS-CoV-2 spike-specific IgG response with neutralisation capacity. In this  
75 series of experiments, we compared the immune response induced by heterologous,  
76 homologous and single dose vaccination with ChAd and saRNA vaccine modalities.  
77 Heterologous vaccination with either ChAd or saRNA prime and alternative boost (i.e. ChAd-  
78 saRNA or saRNA-ChAd) or two doses of saRNA induced the highest IgG responses, compared  
79 to mice vaccinated with a single dose of either ChAd or saRNA (Fig. 1A and Fig. S1A), with  
80 strong correlation between the two independent IgG ELISA methods (Fig. S1B). This IgG  
81 response showed mixed profile, with mainly IgG2 (IgG2a, IgG2b in both mouse strains and  
82 IgG2c in CD1 mice) and IgG1 subclasses (in both mouse strains) (Fig. 2A and B), which was  
83 similar to previously reported results after vaccination with ChAd alone (Silva-Cayetano in  
84 press) or saRNA alone<sup>3</sup>.  
85 Comparable amounts of SARS-CoV-2 spike-specific IgM were detected in all vaccinated  
86 groups (Fig. 1B), while heterologous vaccination with saRNA-ChAd induced higher serum  
87 SARS-CoV-2 spike-specific IgA levels compared to single vaccination with either vaccine, in  
88 both CD1 and BALB/c mice (Fig. 1B).  
89 Two doses of vaccine were also shown to increase the avidity of the IgG towards SARS-CoV-  
90 2 spike (Fig. 1C) compared to single administration of either vaccine, while antibody-  
91 mediated neutralisation was measured across all groups of vaccinated mice, with  
92 heterologous and two dose saRNA inducing significantly higher levels of neutralisation  
93 compared to single dose vaccination regimens (Fig. 1D). Not surprisingly, a correlation was

94 measured between neutralisation and levels of IgG /IgA SARS-CoV-2 spike-specific  
95 antibodies (Fig. S1C).  
96 Flow cytometry staining enabled identification of SARS-CoV-2 spike-specific B cells in the  
97 spleen of mice. The data demonstrated that all vaccination regimens induced a similar  
98 number of antigen specific B cells (Fig. S2B), with similar numbers of germinal centre (GC)  
99 and isotype class switched B cells observed in all groups of vaccinated mice.

100

### 101 **Heterologous vaccination induces strong Th1 type response**

102 Cell mediated immunity was also investigated following heterologous or homologous  
103 ChAdOx1 and saRNA vaccination regimens. The highest IFN $\gamma$  response detected by ELISpot  
104 was observed in mice that received a heterologous combination of vaccines, this increase  
105 was only statistically significant when compared to single administration of saRNA in both  
106 strains of mice (Fig. 3A and B), or saRNA-ChAd compared to ChAd in BALB/c mice (Fig. 3B). In  
107 agreement with earlier reports, ELISpot responses were primarily directed towards the S1  
108 portion of the spike protein (Fig S3A), with a consistent breadth of response measured with  
109 all vaccine combinations and in both strains of mice (Fig. 3A and B).

110 Phenotype and functional capacity of the T cell response was measured by intracellular  
111 cytokine staining, together with memory T cell marker staining. Consistent with previously  
112 published data, saRNA and ChAd vectors induced antigen specific CD4<sup>+</sup> T cells of a Th1 bias,  
113 with minimal IL4 and IL10 production measured and a response dominated by production of  
114 IFN $\gamma$  and TNF $\alpha$ , regardless of the vaccination regimen (Fig. 4A). Antigen specific CD4<sup>+</sup> T cells  
115 displayed mixed Teff and Tem phenotype, with no statistically significant differences  
116 observed in the total number of cells (Fig. 4A) and cell subsets (Fig. S3C). As before, in mice  
117 the cell-mediated response following vaccination was dominated by CD8<sup>+</sup> T cells, with much

118 higher levels of IFN $\gamma$  and TNF $\alpha$  (in addition to upregulation of CD107a) seen in all vaccine  
119 groups (Fig. 4B) compared to CD4 $^{+}$  T cell responses. In addition, the highest frequency of  
120 antigen specific cells, in both outbred and inbred strains of mice, was measured following  
121 heterologous vaccination, regardless of vaccine order (Fig. 4B). Antigen specific CD8 $^{+}$  T cells  
122 displayed a predominantly Teff phenotype, with the highest number of total antigen specific  
123 cells (Fig. 4B) observed in heterologous vaccinated animals.

124

125

126 **Discussion**

127 The current pandemic and extraordinary efforts to develop effective vaccines with  
128 subsequent mass vaccination roll-out has highlighted the ‘real-world’ practicalities of global  
129 vaccination campaigns. There are around 20 vaccines in Phase 3 clinical trial assessment,  
130 and several vaccines have already reported efficacy with subsequent emergency licensure  
131 granted in some countries. While each individual vaccine candidate has been thoroughly  
132 tested for safety and efficacy, there have been no studies reported to date that have  
133 examined the safety, efficacy or any added benefit of mixed modality vaccinations. Given  
134 the real-world vaccination initiatives that are being progressed, there may be a scenario  
135 wherein an individual receives a vaccine prime and a boost dose from different  
136 manufacturers or of different vaccine types. This current pre-clinical study examined the  
137 cellular and humoral immune responses in mice following vaccination with either the  
138 ChAdOx adenoviral vector or the saRNA LNP in homologous or heterologous prime-boost  
139 combinations and compared immunogenicity to single moiety vaccinations.

140

141 All prime-boost regimens elicited high levels of SARS-CoV-2 spike-specific antibodies with  
142 neutralisation capacity and high avidity, levels that were greater than single vaccines alone.  
143 While heterologous vaccination regimens induced the highest antibody responses post-  
144 vaccination, homologous saRNA and ChAd induced higher antibody responses than single  
145 dose regimens, consistent with previous data in mice, pigs and NHPs<sup>11,12</sup>. Importantly in  
146 human clinical trials, strong enhancement of the antibody response was observed following  
147 a booster dose of ChAdOx1<sup>13</sup>, with this regimen shown to provide efficacy against SARS-  
148 CoV-2 disease in late-stage clinical trials<sup>8</sup>. The cell-mediated response was dominated by  
149 cytotoxic T cells, with heterologous regimens inducing higher frequencies and total numbers

150 of antigen specific CD8<sup>+</sup> T cells. Although CD4<sup>+</sup> T cell responses were overall lower in  
151 frequency and number than CD8<sup>+</sup> T cell responses, all vaccination regimens elicited CD4<sup>+</sup> T  
152 cell responses of a Th1 type response, even in the Th2 biased BALB/c background, a  
153 response indicating that the potential for antibody dependent enhancement (ADE) and  
154 subsequent enhancement of respiratory disease (ERD) caused by Th2-type lung  
155 immunopathology is reduced <sup>14-16</sup>.

156

157 While there are no defined correlates of protection, Rhesus Macaques studies have  
158 demonstrated a clear role for neutralising antibodies and also CD8<sup>+</sup> T cells <sup>17</sup>. In agreement,  
159 human studies have demonstrated neutralising antibodies and T cells play an important role  
160 in preventing severe disease and augmenting recovery from COVID-19<sup>18</sup>. Both vaccine  
161 modalities elicited high numbers of antigen specific T cells, which were further increased in  
162 the heterologous regimens. The majority of the IFN $\gamma$  ELISpot response was directed against  
163 the S1 spike protein, particularly the first half (317 AA) which does not include the RBD. Not  
164 surprisingly two doses regimens induced higher antibody responses, with combination  
165 regimens leading to simultaneous high levels of neutralising antibodies and T cell responses.

166

167 Vaccination regimens that induce a broad immune response (humoral and cell-mediated)  
168 will likely be the best option for long-term protection against severe disease and will be best  
169 placed if booster vaccinations are considered in the future. The logistical challenges of  
170 administering vaccines in a rapidly evolving landscape of mass vaccination schemes, coupled  
171 with limited global supply, underpins the need to generate data on mixing vaccine  
172 modalities. The data described herein suggests clinical trials should progress to assess the



173 safety, immunogenicity and efficacy of heterologous vaccination regimens to help progress

174 global deployment and vaccine uptake against SARS-CoV-2.

175

176

177

178 **Methods**

179 **Ethics Statement;** Mice were used in accordance with the UK Animals (Scientific  
180 Procedures) Act under project license number P9804B4F1 granted by the UK Home Office.  
181 Age matched animals were purchased from commercial suppliers as a batch for each  
182 experiment and randomly split into groups on arrival at our facility. Animals were group  
183 housed in IVCs under SPF conditions, with constant temperature and humidity with lighting  
184 on a 13:11 light-dark cycle (7am to 8pm). For induction of short-term anaesthesia, animals  
185 were anaesthetised using vaporised IsoFlo<sup>®</sup>. All animals were humanely sacrificed at the end  
186 of each experiment by an approved Schedule 1 method.

187

188 **Animals and Immunizations;** Outbred CD1Hsd:ICR (CD-1) (Envigo) (n=8 per group), Crl:CD1  
189 (ICR) (Charles River) (n=8 per group) and inbred BALB/cOlaHsd (BALB/c) (Envigo) (n=6 per  
190 group) mice of 7 weeks of age, were immunized intramuscularly (i.m.) in the musculus  
191 tibialis with 10<sup>8</sup> infectious units (iu) of ChAdOx1 nCoV-19<sup>12</sup> or 1 $\mu$ g saRNA<sup>3</sup>. Mice were  
192 boosted i.m. with the relevant vaccine candidate 4 weeks later. All mice were sacrificed 3  
193 weeks after the final vaccination with serum and spleens collected for analysis of humoral  
194 and cell-mediated immunity.

195

196 **Pseudotype virus neutralisation assay;** A HIV-pseudotyped luciferase-reporter based  
197 system was used to assess the neutralization ability of sera from vaccinated mice. In brief,  
198 CoV S-pseudotyped viruses were produced by co- transfection of 293T/17 cells with a HIV-1  
199 gag-pol plasmid (pCMV- $\Delta$ 8.91, a kind gift from Prof. Julian Ma, St George's University of  
200 London), a firefly luciferase reporter plasmid (pCSFLW, a kind gift from Prof. Julian Ma, St  
201 George's University of London) and a plasmid encoding the S protein of interest (pSARS-

202 CoV2-S) at a ratio of 1:1.5:1. Virus- containing medium was clarified by centrifugation and  
203 filtered through a 0.45 µm membrane 72 h after transfection, and subsequently aliquoted  
204 and stored at –80 °C. For the neutralization assay, heat-inactivated sera were first serially  
205 diluted and incubated with virus for 1 h, and then the serum-virus mixture was transferred  
206 into wells pre-seeded Caco2 cells. After 48 h, cells were lysed, and luciferase activity was  
207 measured using Bright-Glo Luciferase Assay System (Promega). The IC50 neutralization was  
208 then calculated using GraphPad Prism (version 8.4). Statistical analyses were performed on  
209 log transformed data.

210

211 **Antigen-specific IgG ELISA;** The antigen-specific IgG titres in mouse sera were assessed by a  
212 semi-quantative ELISA. MaxiSorp high binding ELISA plates (Nunc) were coated with 100 µL  
213 per well of 1 µg mL<sup>-1</sup> recombinant SARS-CoV-2 protein with the pre-fusion stabilized  
214 conformation in PBS. After overnight incubation at 4 °C, the plates were washed 4 times  
215 with PBS-Tween 20 0.05% (v/v) and blocked for 1 h at 37 °C with 200 µL per well blocking  
216 buffer (1% BSA (w/v) in PBS-Tween-20 0.05%(v/ v)). The plates were then washed and the  
217 diluted samples or a 5-fold dilution series of the standard IgG added using 50 µL per well  
218 volume. Plates were incubated for 1 h at 37 °C, then washed and secondary antibody added  
219 at 1:2000 dilution in blocking buffer (100 µL per well) and incubated for 1 hr at 37 °C. After  
220 incubation and washes, plates were developed using 50 µL per well SureBlue TMB (3,3', 5,5'-  
221 tetramethylbenzidine) substrate and the reaction stopped after 5 min with 50 µL per well  
222 stop solution (Insight Biotechnologies). The absorbance was read on a Versamax  
223 Spectrophotometer at 450 nm (BioTek Industries). Statistical analyses were performed on  
224 log-transformed data.

225

226 **Antigen specific Isotype ELISA;** MaxiSorp plates (Nunc) were coated with 50  $\mu$ L of 2  $\mu$ g/mL  
227 or 50  $\mu$ L of 5  $\mu$ g/mL ng/well SARS-CoV-2 FL-S protein overnight at 4 °C for detection of IgG  
228 (250ng/well) or IgM and IgA (500ng/well), respectively, prior to washing in PBS/Tween  
229 (0.05% v/v) and blocking with Blocker Casein in PBS (Thermo Fisher Scientific) for 1 h at  
230 room temperature (RT). Standard positive serum (pool of mouse serum with high endpoint  
231 titre against FL-S protein), individual mouse serum samples, negative and an internal control  
232 (diluted in casein) were incubated for 2 hrs at room temperature for detection of specific  
233 IgG or 1h at 37 °C for detection of specific IgM or IgA. Following washing, bound antibodies  
234 were detected by addition of alkaline phosphatase (AP)-conjugated goat anti-mouse IgG  
235 (Sigma-Aldrich) or anti-mouse IgM (Abcam) or anti-mouse IgA (SouthernBiotech) for 1h at  
236 room temperature and addition of p-Nitrophenyl Phosphate, Disodium Salt substrate  
237 (Sigma-Aldrich). An arbitrary number of ELISA units (EU) were assigned to the reference  
238 pool and optical density values of each dilution were fitted to a 4-parameter logistic curve  
239 using SOFTmax PRO software. ELISA units were calculated for each sample using the optical  
240 density values of the sample and the parameters of the standard curve. IgM limit of  
241 detection was defined a 2 ELISA Units, IgA limit of detection set as 6 ELISA Units. All data  
242 was log-transformed for statistical analyses.

243

244 **Antigen Specific IgG Subclass ELISAs;** MaxiSorp plates (Nunc) were coated with 50  $\mu$ L of 2  
245  $\mu$ g/mL per well of SARS-CoV-2 FL-S protein overnight at 4 °C prior to washing in PBS/Tween  
246 (0.05% v/v) and blocking with Blocker Casein in PBS (Thermo Fisher Scientific) for 1 h at  
247 room temperature (RT). For detection of IgG subclasses all serum samples were diluted to 1  
248 total IgG EU and incubated at 37 °C for 1 h prior to detection with Alkaline Phosphatase  
249 conjugated anti-mouse IgG subclass-specific secondary antibodies (Southern Biotech or

250 Abcam) incubated for 1 h at 37 °C . The results of the IgG subclass ELISA are presented using  
251 optical density values.

252

253 **Avidity ELISA;** Anti-SARS-CoV-2 spike-specific total IgG antibody avidity was assessed by  
254 sodium thiocyanate (NaSCN)-displacement ELISA. Nunc MaxiSorp ELISA plates (Thermo  
255 Fisher Scientific) coated overnight at 4 °C with 2µg/well SARS-CoV-2 trimeric spike protein  
256 diluted in PBS were washed with PBS/Tween (0.05% v/v) and blocked for 1 h with 100 µl per  
257 well of Blocker Casein in PBS (Thermo Fisher Scientific) at 20 °C. Test samples and a positive  
258 control serum pool were diluted in blocking buffer to 1 total IgG EU and incubated for 2 h at  
259 20 °C. After washing, increasing concentrations of NaSCN (Sigma-Aldrich) diluted in PBS  
260 were added and incubated for 15 min at 20 °C. Following another wash, bound antibodies  
261 were detected by addition of AP-conjugated goat anti-mouse IgG (Sigma-Aldrich) for 1 h at  
262 room temperature and addition of p-Nitrophenyl Phosphate, Disodium Salt substrate  
263 (Sigma-Aldrich). For each sample, concentration of NaSCN required to reduce the OD405 to  
264 50% of that without NaSCN (IC50) was interpolated from this function and reported as a  
265 measure of avidity.

266

267 **Antigen specific B cell staining;** Spike, RBD and a decoy NANP<sub>9</sub>C (repeat region from *P.*  
268 *falciparum* CSP protein) tetramers were prepared in house by mixing biotinylated proteins  
269 with streptavidin conjugated flurochromes (A488, A647 or r-PE) in a 4:1 molar ratio and  
270 incubating on ice for 30 minutes. Splenocytes were stained with Spike-PE and RBD-A647 at a  
271 final concentration of 0.04mM, whilst decoy tetramer, NANP<sub>9</sub>C-A488 was used at a final  
272 concentration of 0.4mM. Splenocytes were stained with Live-Dead Aqua and Fc block (anti-  
273 CD16/32 mAb, Clone 93) prior to staining with the antibody cocktail containing NANP<sub>9</sub>C-

274 Alexa488, GL7-PerCPCy5.5 (Clone GL7), CD138 BV421 (Clone 281-2), CD95-BV605 (Clone  
275 SA367H8), CD4-BV650 (Clone GK1.5), CD279-BV711 (Clone 29F.1A12), CD19-BV780 (6D5),  
276 RBD-A647, IgD-A700 (Clone 11-26c.2a), IgM-APCCy7 (Clone 11/41), Spike-PE, CD38-PECY5  
277 (Clone 90), CD69 PeCy7 (Clone H1.2F3), CD45R-BUV395 (Clone RA3-6B2) and CD3-BUV496  
278 (Clone 145-2C11), antibodies purchased from BioLegend, BD or Invitrogen. Antigen specific  
279 B cells were identified by gating on LIVE/DEAD negative, doublet negative (FSC-H vs FSC-A),  
280 size (FSC-H vs SSC), CD45RA<sup>+</sup>, CD19<sup>+</sup> and NANP-A488<sup>-</sup>, RBD-A647<sup>+</sup> and Spike-PE<sup>+</sup>.

281

282 **ELISpot and ICS staining;** Spleen single cell suspension were prepared by passing cells  
283 through 70µM cell strainers and ACK lysis prior to resuspension in complete media. For  
284 analysis of IFN $\gamma$  production by ELISpot, splenocytes were stimulated with two pools of S1  
285 (pools 1 and 2) and two pools S2 (pools 3 and 4) peptides (final concentration of 2µg/mL) on  
286 IPVH-membrane plates (Millipore) coated with 5µg/mL anti-mouse IFN $\gamma$  (AN18). After 18-20  
287 hours of stimulation at 37 °C, IFN $\gamma$  spot forming cells (SFC) were detected by staining  
288 membranes with anti-mouse IFN $\gamma$  biotin (1mg/mL) (R46A2) followed by streptavidin-  
289 Alkaline Phosphatase (1mg/mL) and development with AP conjugate substrate kit (BioRad,  
290 UK).

291 For analysis of intracellular cytokine production, cells were stimulated at 37 °C for 6 hours  
292 with 2µg/mL a pool of S1 (ELISpot pools 1 and 2) or S2 (ELISpot pools 3 and 4) peptides,  
293 media or positive control cell stimulation cocktail (containing PMA-Ionomycin, BioLegend),  
294 together with 1µg/mL Golgi-plug (BD) and 2µl/mL CD107a-Alexa647 (Clone 1D4B). Following  
295 surface staining with CD3-A700 (Clone 17A2), CD4-BUV496 (Clone GK1.5), CD8-BUV496  
296 (Clone 53-6.7), CD44-BV780 (Clone IM7), CD62L-BV711 (Clone MEL-14), CD69-PECy7 (Clone  
297 H1.2F3) and CD127-BV650 (Clone A7R34) or CD127-APCCy7 (Clone A7R34), cells were fixed

298 with 4% paraformaldehyde and stained intracellularly with TNF $\alpha$ -A488 (Clone MP6-XT22),  
299 IL2-PerCPy5.5 (Clone JES6-5H4), IL4-BV605 (Clone 11B11), IL10-PE (Clone JES5-16E3) and  
300 IFN $\gamma$ -e450 (Clone XMG1.2) diluted in Perm-Wash buffer (BD). Sample acquisition was  
301 performed on a Fortessa (BD) and data analyzed in FlowJo V10 (TreeStar). An acquisition  
302 threshold was set at a minimum of 5000 events in the live CD3<sup>+</sup> gate. Antigen specific T cells  
303 were identified by gating on LIVE/DEAD negative, doublet negative (FSC-H vs FSC-A), size  
304 (FSC-H vs SSC), CD3<sup>+</sup>, CD4<sup>+</sup> or CD8<sup>+</sup> cells and cytokine positive. Cytokine positive responses  
305 are presented after subtraction of the background response detected in the corresponding  
306 media stimulated control sample for each mouse and summing together the response  
307 detected to each pool of peptides. T effector (Teff) cells were defined as CD62L<sup>-</sup> CD127<sup>-</sup>, T  
308 central memory cells defined as CD62L<sup>-</sup> CD127<sup>+</sup> and T central memory (Tcm) cells defined as  
309 CD62L<sup>hi</sup> CD127<sup>hi</sup> (Figure S3B). All graphs and statistical analysis were performed using Prism  
310 v9 (Graphpad), total cell counts were log transformed prior to statistical analysis.

311

## 312 **References**

- 313 1 Tregoning, J. S. *et al.* Vaccines for COVID-19. *Clin Exp Immunol* **202**, 162-192,  
314 doi:10.1111/cei.13517 (2020).
- 315 2 Blakney, A. K. *et al.* Big Is Beautiful: Enhanced saRNA Delivery and Immunogenicity  
316 by a Higher Molecular Weight, Bioreducible, Cationic Polymer. *ACS Nano* **14**, 5711-  
317 5727, doi:10.1021/acsnano.0c00326 (2020).
- 318 3 McKay, P. F. *et al.* Self-amplifying RNA SARS-CoV-2 lipid nanoparticle vaccine  
319 candidate induces high neutralizing antibody titers in mice. *Nature communications*  
320 **11**, 3523, doi:10.1038/s41467-020-17409-9 (2020).
- 321 4 Ewer, K. *et al.* Chimpanzee adenoviral vectors as vaccines for outbreak pathogens.  
322 *Hum Vaccin Immunother* **13**, 3020-3032, doi:10.1080/21645515.2017.1383575  
323 (2017).
- 324 5 Antrobus, R. D. *et al.* Clinical assessment of a novel recombinant simian adenovirus  
325 ChAdOx1 as a vectored vaccine expressing conserved Influenza A antigens. *Mol Ther*  
326 **22**, 668-674, doi:10.1038/mt.2013.284 (2014).
- 327 6 Venkatraman, N. *et al.* Safety and Immunogenicity of a Heterologous Prime-Boost  
328 Ebola Virus Vaccine Regimen in Healthy Adults in the United Kingdom and Senegal. *J*  
329 *Infect Dis* **219**, 1187-1197, doi:10.1093/infdis/jiy639 (2019).

- 330 7 Folegatti, P. M. *et al.* Safety and immunogenicity of a candidate Middle East  
331 respiratory syndrome coronavirus viral-vectored vaccine: a dose-escalation, open-  
332 label, non-randomised, uncontrolled, phase 1 trial. *Lancet Infect Dis* **20**, 816-826,  
333 doi:10.1016/S1473-3099(20)30160-2 (2020).
- 334 8 Voysey, M. *et al.* Safety and efficacy of the ChAdOx1 nCoV-19 vaccine (AZD1222)  
335 against SARS-CoV-2: an interim analysis of four randomised controlled trials in Brazil,  
336 South Africa, and the UK. *Lancet* **397**, 99-111, doi:10.1016/S0140-6736(20)32661-1  
337 (2021).
- 338 9 Ewer, K. J. *et al.* T cell and antibody responses induced by a single dose of ChAdOx1  
339 nCoV-19 (AZD1222) vaccine in a phase 1/2 clinical trial. *Nat Med*,  
340 doi:10.1038/s41591-020-01194-5 (2020).
- 341 10 Barrett, J. R. *et al.* Phase 1/2 trial of SARS-CoV-2 vaccine ChAdOx1 nCoV-19 with a  
342 booster dose induces multifunctional antibody responses. *Nat Med*,  
343 doi:10.1038/s41591-020-01179-4 (2020).
- 344 11 Graham, S. P. *et al.* Evaluation of the immunogenicity of prime-boost vaccination  
345 with the replication-deficient viral vectored COVID-19 vaccine candidate ChAdOx1  
346 nCoV-19. *NPJ Vaccines* **5**, 69, doi:10.1038/s41541-020-00221-3 (2020).
- 347 12 van Doremalen, N. *et al.* ChAdOx1 nCoV-19 vaccine prevents SARS-CoV-2 pneumonia  
348 in rhesus macaques. *Nature* **586**, 578-582, doi:10.1038/s41586-020-2608-y (2020).
- 349 13 Ramasamy, M. N. *et al.* Safety and immunogenicity of ChAdOx1 nCoV-19 vaccine  
350 administered in a prime-boost regimen in young and old adults (COV002): a single-  
351 blind, randomised, controlled, phase 2/3 trial. *Lancet* **396**, 1979-1993,  
352 doi:10.1016/S0140-6736(20)32466-1 (2021).
- 353 14 Wang, S. F. *et al.* Antibody-dependent SARS coronavirus infection is mediated by  
354 antibodies against spike proteins. *Biochem Biophys Res Commun* **451**, 208-214,  
355 doi:10.1016/j.bbrc.2014.07.090 (2014).
- 356 15 Tseng, C. T. *et al.* Immunization with SARS coronavirus vaccines leads to pulmonary  
357 immunopathology on challenge with the SARS virus. *PLoS One* **7**, e35421,  
358 doi:10.1371/journal.pone.0035421 (2012).
- 359 16 Lee, W. S., Wheatley, A. K., Kent, S. J. & DeKosky, B. J. Antibody-dependent  
360 enhancement and SARS-CoV-2 vaccines and therapies. *Nat Microbiol* **5**, 1185-1191,  
361 doi:10.1038/s41564-020-00789-5 (2020).
- 362 17 Mercado, N. B. *et al.* Single-shot Ad26 vaccine protects against SARS-CoV-2 in rhesus  
363 macaques. *Nature* **586**, 583-588, doi:10.1038/s41586-020-2607-z (2020).
- 364 18 Rydzynski Moderbacher, C. *et al.* Antigen-Specific Adaptive Immunity to SARS-CoV-2  
365 in Acute COVID-19 and Associations with Age and Disease Severity. *Cell* **183**, 996-  
366 1012 e1019, doi:10.1016/j.cell.2020.09.038 (2020).

367

368 **Acknowledgments:** The authors would like to thank D. Pulido for provision of spike and RBD  
369 proteins, BMS staff for animal husbandry and management and A. Worth, J. Furze, M.  
370 Mykhaylyk and R. Evans for facilities support.

371



372 **Funding:** This report is independent research funded by the National Institute for Health  
373 Research (UKRI Grant Ref: MC\_PC\_19055, NIHR Ref: COV19 OxfordVacc-01). The views  
374 expressed in this publication are those of the author(s) and not necessarily those of the  
375 National Institute for Health Research or the Department of Health and Social Care.

376

377 **Author Contributions:** AJS, MU, SB-J, CB, KS, KM & PMK performed experiments. AJS, MU,  
378 HS, CG, EA & AT performed animal procedures and/or sample processing. AJS, SBJ, KH &  
379 PMK, analyzed data. AJS, TL, PMK, RS & SG designed the study. AJS, SBJ, TB wrote the  
380 manuscript. All authors reviewed the final version of the manuscript.

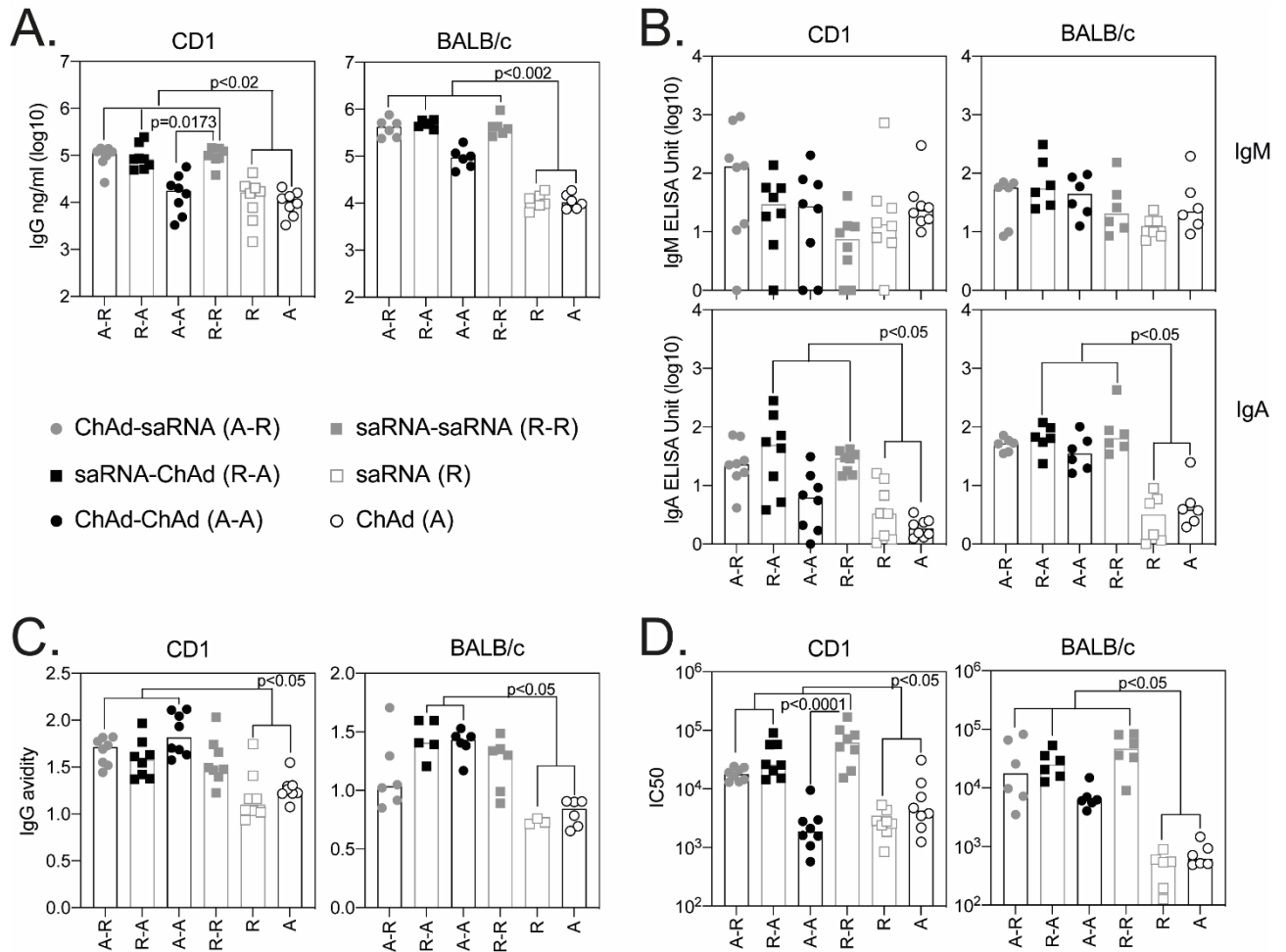
381

382 **Competing interests:** SCG is co-founder and board member of Vaccitech (collaborators in  
383 the early development of this vaccine candidate) and named as an inventor on a patent  
384 covering use of ChAdOx1-vectored vaccines and a patent application covering this SARS-  
385 CoV-2 vaccine. TL is named as an inventor on a patent application covering this SARS-CoV-2  
386 vaccine and was consultant to Vaccitech. PMK and RJS are co-founders and RJS is a board  
387 member of VaxEquity and VacEquity and are named inventors on a patent application  
388 covering the SARS-CoV-2 saRNA vaccine candidate.

389

390

391 **Figure legends**



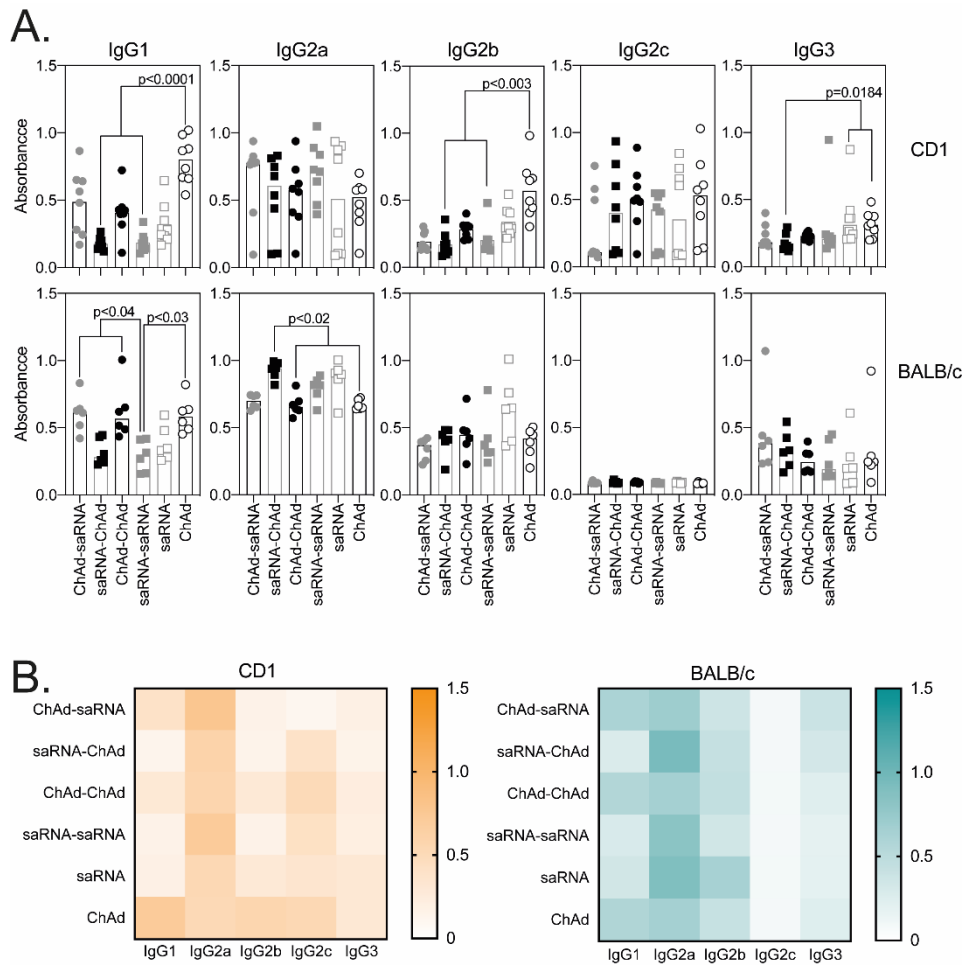
392

393 **Fig 1: Antibody responses following ChAd and saRNA vaccination**

394 Antibody responses were measured in the serum of mice collected 3 weeks after the final  
395 immunisation. Graphs show SARS CoV-2 spike-specific IgG (A.), IgM and IgA (B.) and IgG  
396 avidity (C.) measured by ELISA, and SARS-CoV-2 pseudotyped virus neutralisation (IC<sub>50</sub>) (D.).  
397 Individual mice are represented by a single data point, bars represent the median response  
398 in each group (CD1 n=8; BALB/c n=6). Data in each graph was analysed with a Kruskal-Wallis  
399 and post-hoc positive test to compare differences between vaccination groups, p values  
400 indicate significant differences between groups.

401

402



403

404 **Fig 2: SARS-CoV-2 spike-specific IgG subclasses following ChAd and saRNA vaccination**

405 For detection of IgG subclasses, each sample was diluted to 1 IgG ELISA Unit. Graphs show

406 optical density measured against each IgG subclass where individual data points were

407 expressed as an OD and shown here as scatter dot plots with bars showing the median (**A.**),

408 followed by the heatmap summary representation with median response in each group to

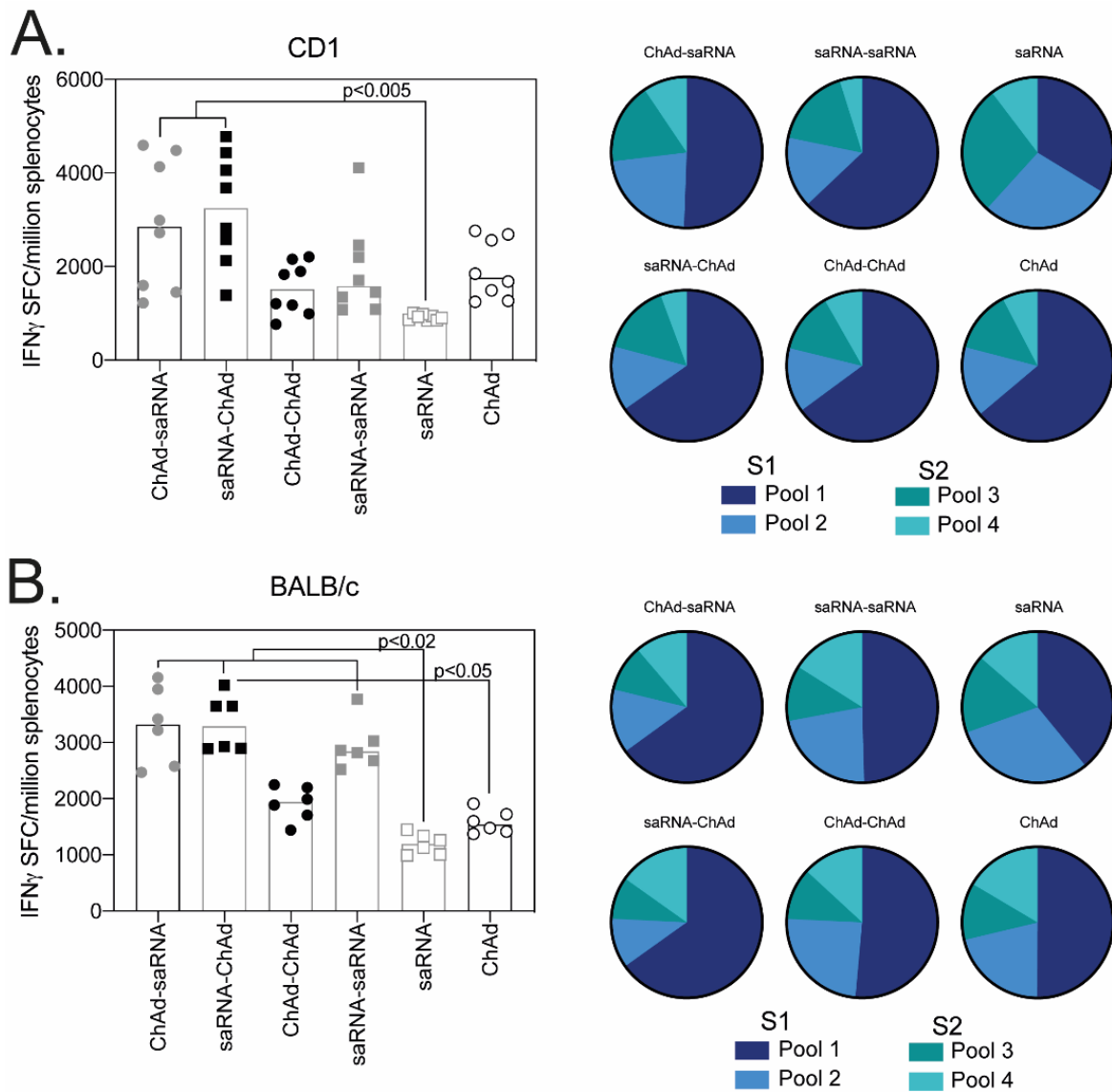
409 each IgG subclass (**B.**). Individual mice are represented by a single data point, bars represent

410 the median response in each group (CD1 n=8; BALB/c n=6). Data in each graph was analysed

411 with a Kruskal-Wallis and post-hoc positive test to compare differences between vaccination

412 groups, p-values indicate significant differences between groups.

413



414

415 **Fig 3: Breadth of T cell response measured by ELISpot**

416 Graphs represent the total spike specific IFN $\gamma$  response (sum of peptide pools) measured in

417 outbred CD1 (**A.**) or inbred BALB/c (**B.**). Pie charts represent the response to each peptide

418 pool as a proportion of total response. Data points represent individual mice and bars

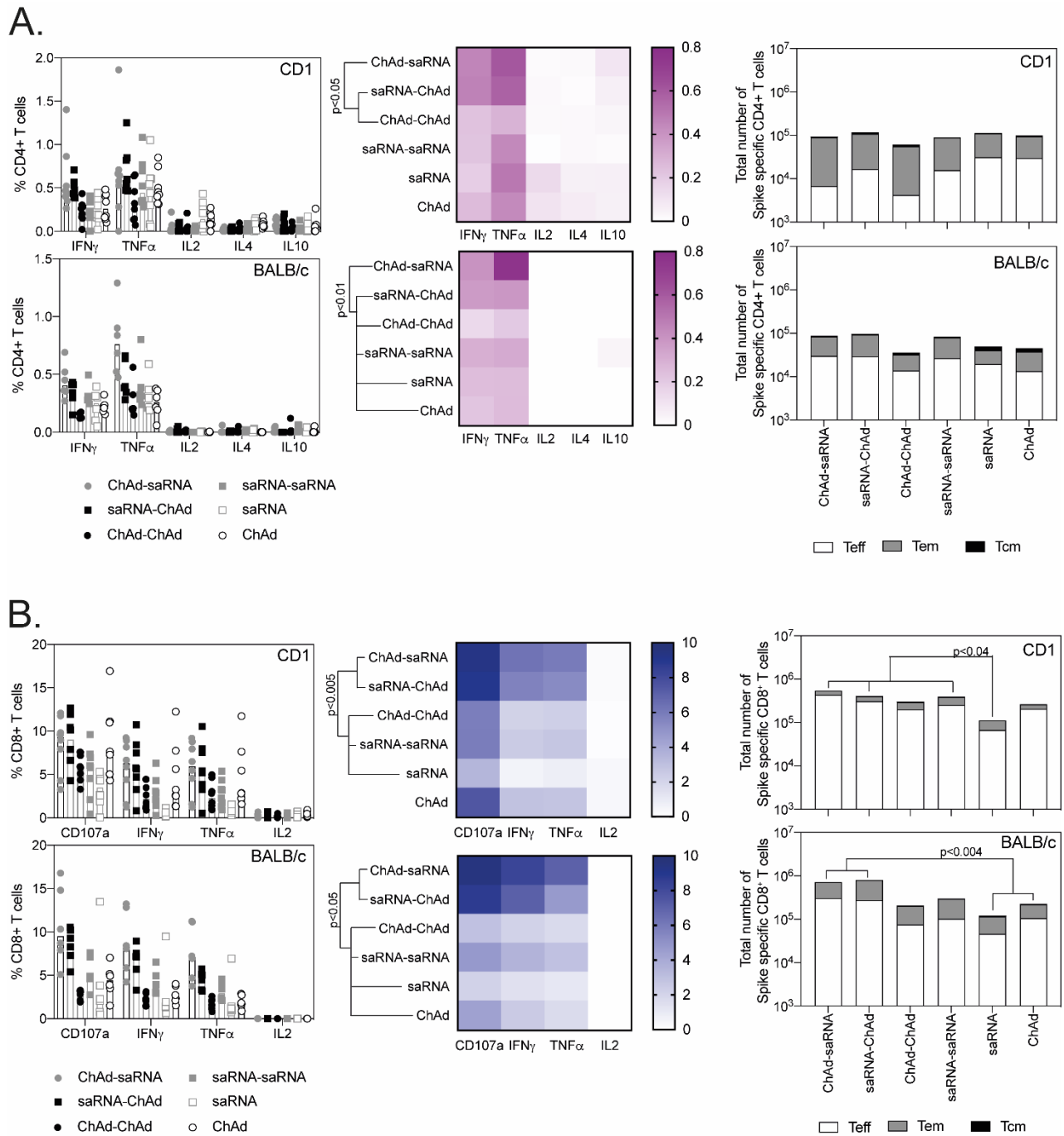
419 represent the median response in each group. Data in each graph was analysed with a

420 Friedman test and post-hoc Dunn's multiple comparison to compare between vaccination

421 regimens, p values are indicated on the graph.

422

423

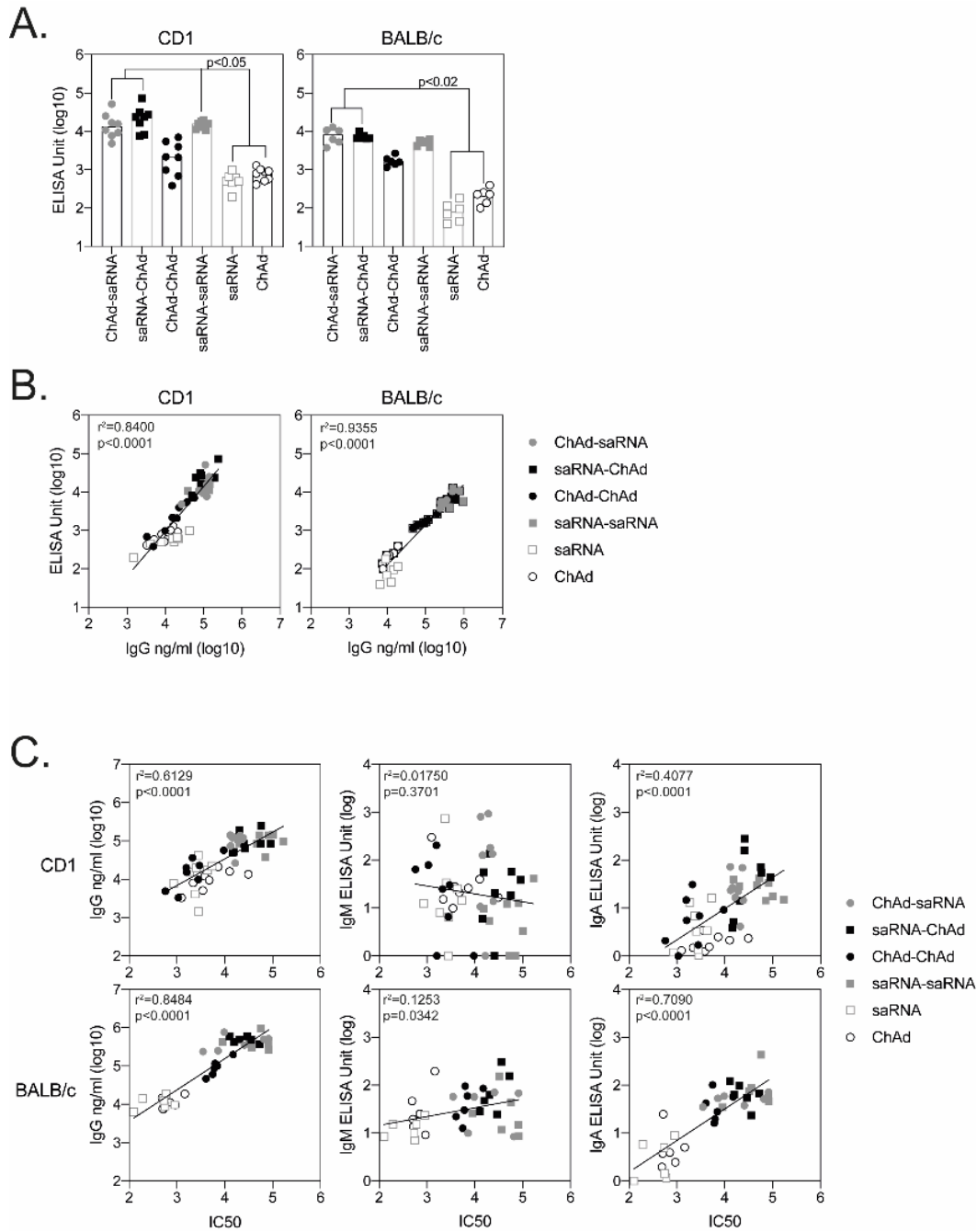


430 each cytokine and total number of antigen specific cells of a T effector (Teff), T effector  
431 memory (Tem) or T central memory (Tcm) phenotype (right). **B.**) Graphs show the  
432 frequency of the spike-specific CD8<sup>+</sup> T cells responses (left) in CD1 (top panel; n=8) and  
433 BALB/c mice (bottom panel; n=6), heatmaps (middle) show the proportion of the response  
434 producing each cytokine and total number of antigen specific cells of a T effector (Teff), T  
435 effector memory (Tem) or T central memory (Tcm) phenotype (right). Data points indicate  
436 individual mice, bars represent the median response in each group. Total numbers of each  
437 population are displayed in Fig S3C. Data in each graph was analysed with a two-way anova  
438 and post-hoc Tukey's multiple comparison test to compare between vaccination regimens, p  
439 values are indicated on the graph.

440

441

442



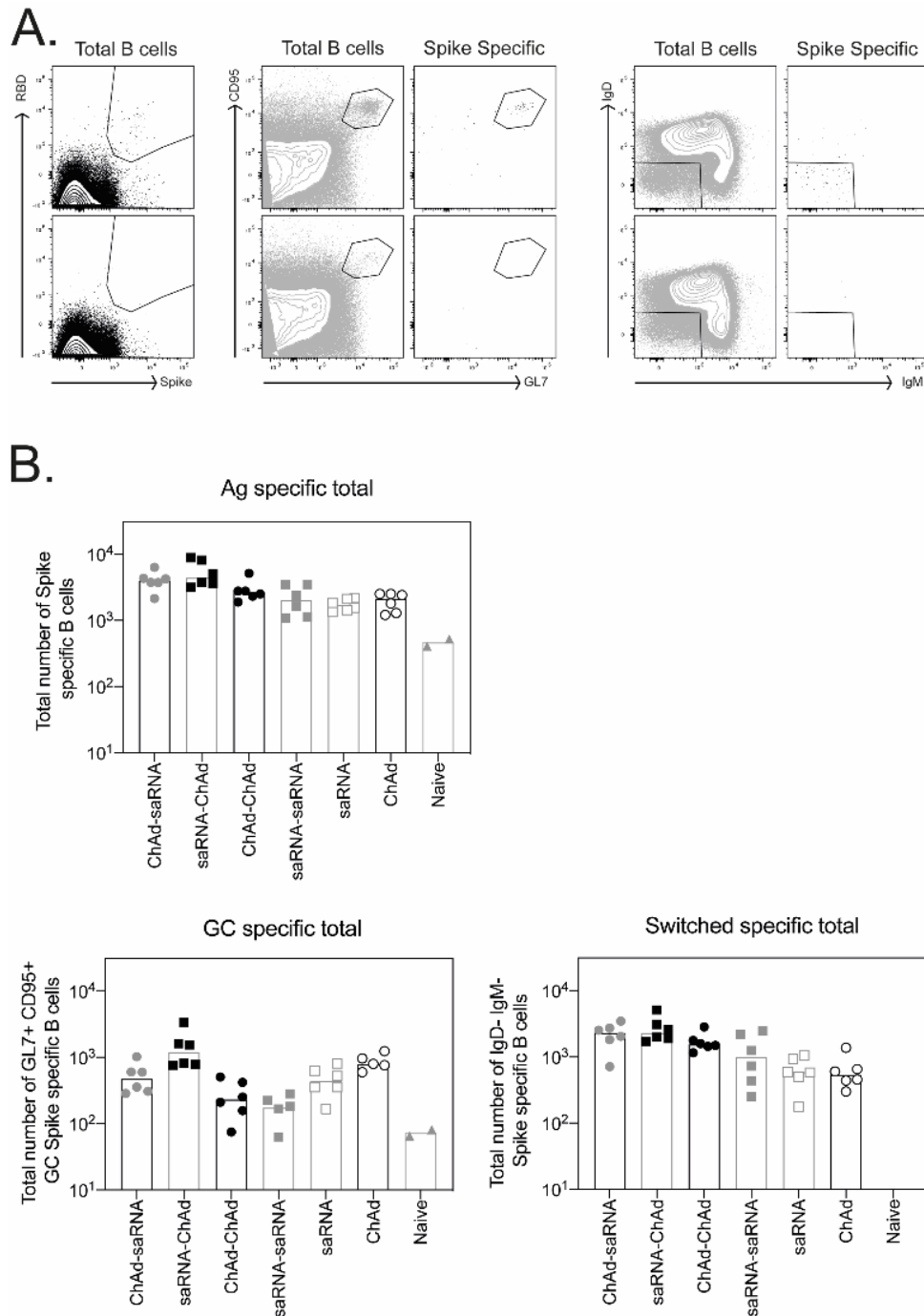
450 regression on log-transformed values. Data points represent individual animals from all

451 groups together,  $r^2$  and p values are indicated on each graph.

452

453





454

455 **Fig S2: Antigen specific B cell responses**

456 SARS-CoV-2 spike-specific B cells responses were measured in the spleen of BALB/c mice 3

457 weeks after the final immunisation. **A.)** Antigen specific cells were identified by staining with

458 spike-PE and RBD-A647 tetramers. Germinal center (GC) B cells were identified as GL7+,

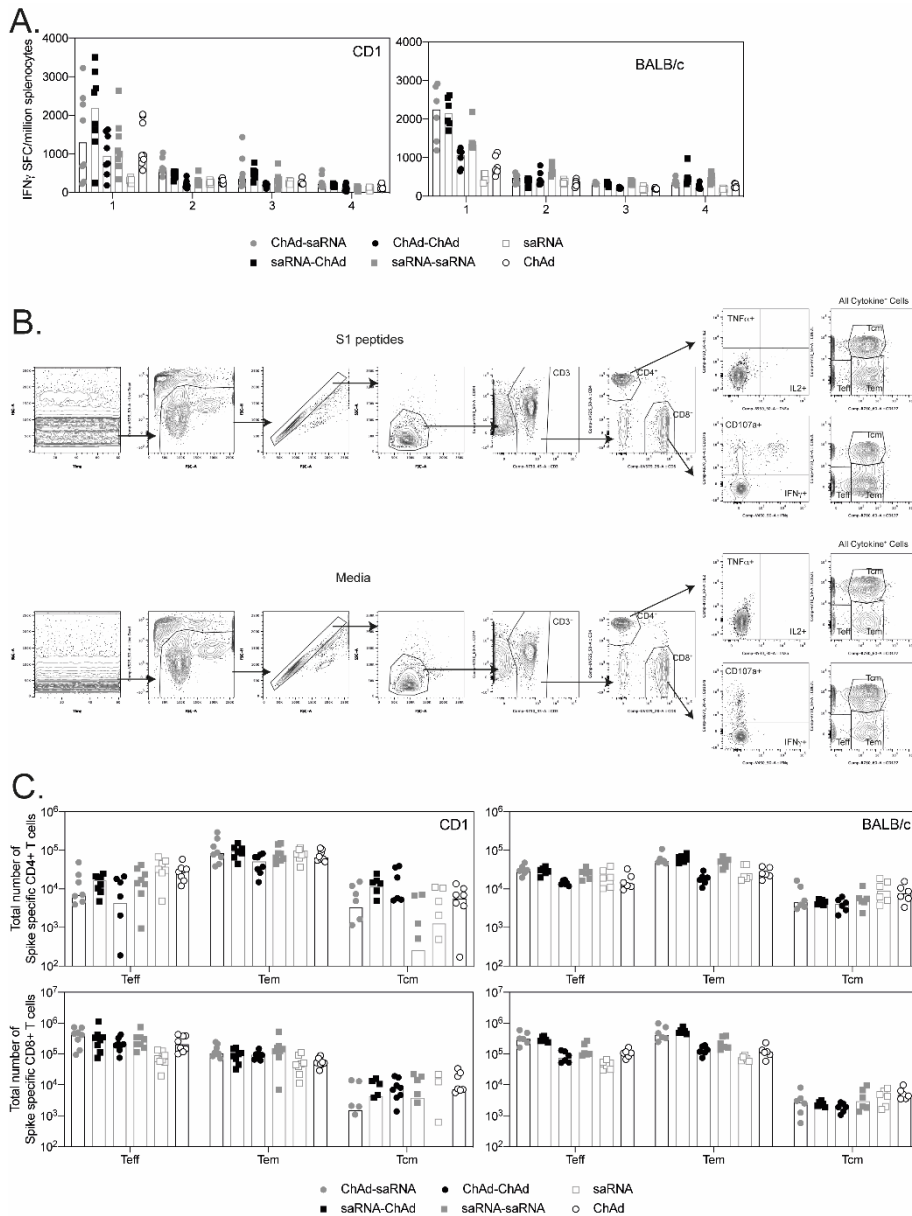
459 CD95+, switched B cells identified as IgD- and IgM- antigen-specific B cells **B.)** Graphs show

460 the total number of antigen-specific B cells, antigen-specific GC B cells and antigen-specific

461 switched B cells, data points are representative of individual mice, median responses per

462 group indicated by bars.

463



464

465 **Fig S3: T cell responses measured by ELISpot and ICS**

466 **A.)** Graphs show the IFN $\gamma$  SFC detected to each pool of peptides by ELISpot. Each data point  
467 represents an individual mouse, bars represent the median response per group.

468 **B.)** Plots show the gating strategy used to identify antigen specific T cell responses.

469 **C.)** Graphs show the total number of Teff, Tem and Tcm responses detected in the spleens

470 of mice. Each point indicates an individual mouse, bars represent the median response per

471 group.

472